Chalcogenide Letters Vol. 12, No. 8, August 2015, p. 415 - 427

PHYSICAL PROPERTIES OF VACUUM EVAPORATED TIN SULFIDE THIN FILMS

J. S. CRUZ[a*], K. MONFIL LEYVA[b], N. R. MATHEWS[b], A. MENDOZA GALVÁN[c], X. MATHEW[b]

[a]*Facultad de Química, Energía-Materiales. Universidad Autónoma de Querétaro, Querétaro, 76010, México*

[b]*Instituto de Energías Renovables, Universidad Nacional Autónoma de México, Temixco, Morelos, 62580, México*

[c]*Centro de Investigación y de Estudios Avanzados, Unidad Querétaro, A.P. 1-798, Querétaro, Qro., 76001, México*

Tin sulfide thin films were grown into vacuum evaporated onto soda lime and conducting glass substrates varying the substrate temperatures in the range of 150 to 350 ^{0}C. The samples were characterized for structure, morphology, optical, and opto-electronic properties. All the thin films showed at Herzenbergite structure with cells parameters close to the powder of SnS. The band gap varied from 1.19 to 1.26 eV as the substrate temperature increased. The grain size showed a very significant dependence on substrate temperature; the average grain size measured for films deposited were 23 to 52 nm. The Raman technique shows that the structure is SnS with traces of the Sn_2S_3 and SnS_2 compounds. The EDS analysis shows the Sn/S ratio in the range of 1.01-1.1. Photosensitivity measurements revealed that films deposited at 300^{0}C have better photoresponse, and the photoconductivity increased after annealing the films, the resistivity values varied of 10^3 to 10^5 Ω-cm with the increase of substrate temperature.

(Received July 1, 2015; Accepted August 17, 2015)

Keywords: SnS, Evaporation, Optical, structural and morphological properties

1. Introduction

Energy is a topic of considerable current interest because of it´s importance in the technological advancement of countries and at the same time in the deterioration of the environment. The use of renewable energy has attracted attention for it has a low impact on environmental pollution. In particular the photovoltaic has been the target of a lot research due to the necessity to find photovoltaic materials environmentally friendly, abundant in the earth crust, quick and easy to obtaining. Tin mono sulfide has particularly generated interest due to physicochemical properties. Several binary phases of tin sulfides are known SnS, SnS_2, Sn_2S_3, Sn_3S_4 and Sn_4S [1], the binary compounds that had been shown good characteristics for application as optoelectronic materials are SnS and SnS_2. The SnS thin films had a band gap that has been reported of the order of 1.65 up to 1.1 eV close to the optimum for solar cells production (1.1-1.6 eV) and high optical absorption coefficient>α10 ^{5} cm^{-1} [2-6] and nontoxic material. Among the theoretical studies, it had been indicated that the solar conversion efficiencies higher than 25 % could be achieved using an SnS semiconductor [7, 8]. Generally this compound crystallizes in the Herzenbergite orthorhombic structure with preferential orientation in the (111) plane and lattice parameters: a=4.3291 Å, b=11.1923 Å and c=3.9838 Å [9]. In order to obtained

*Corresponding autor: jsantos@uaq.edu.mx

SnS thin films the following methods have been used; Hot Injection Technique [10], Spray Pyrolysis [11, 12], Electron Beam Evaporation [13], Evaporation [14], Chemical Bath Deposition [15, 16], SILAR method [17,18], and Electrodeposition [19]. Due to the increasing interest of SnS thin films, the present work attempts to find out conditions of growing SnS thin films with better properties in order to be applied on photovoltaic and solar cell using vacuum evaporation and controlled deposition conditions with attention given to its optical, structural and electrical properties. In this work we report some results on the physical and chemical properties of thin films of SnS obtained by the evaporation technique. It is expected that better understanding of this material, and their optimized device design, will lead to obtained a good solar cells with nontoxic elements.

The evaporation technique is cheap, fast, films are grown of 2-6 μm in 10 to 15 minutes, in this technique, and there exists controls in the polycristallinity, band gap and phase of the SnS films [20, 21]. In the present work we show the characteristics of the deposited SnS polycrystalline thin films obtained by evaporation technique varying the substrate temperature in order to show the future use as absorbent material in solar cells or in new absorbent materials such as Cu_2ZnSnS_4. In the table I we observed the different techniques of preparation and properties of the SnS thin films material.

Table I

Technique	GS/nm	[Sn/S]	E_g/eV	T_S/°C	T_{ann}, Atm/°C	Structure	RMS/nm	Reference
SC	-	-	1.08	RT	-	-	-	[22]
CVD	-	0.89	1-2.3	100	200, air	MP	-	[23]
EV	-	1.002	1.4-2.33	RT	160-300, vac.	HZ	-	[24]
EBE	-	-	1.23-1.38	300	-	HZ	51	[25]
EV	-	-	1.38-2.33	27,150	150, vac.	A, PC	-	[26]
EV	-	-	-	27-300	-	PC	-	[27]
EV	70	1.06	1.35-1.42	300	100-400, vac.	HZ	4.3	[21]
EV	168-220	1.05	1.35-1.86	300	-	HZ	7.83-14.9	[28]
cEV	-	-	1.3-1.6	200-400	-	MP	-	[29]
EV	178-192	-	1.35	275	-	HZ	5.19-13.14	[30]
cEV	50-90	0.96-1.26	1.37	RT-300	200, vac.	MP	-	[31]
EV	75-175	0.875-1.10	1.32-1.68	RT-325	-	MP	-	[20]
EV	30-140	1.01-1.10	1.37-1.60	300	100, vac.	HZ	-	[32]
EV	119-217	0.92-1.78	0.94-1.36	300	-	HZ	8-72	[33]
CBD	-	-	1.12-1.7	RT-35	125-550, N_2	HZ	-	[34]
SILAR	-	1.13	1.43	RT	-	HZ	-	[35]
TD	15	-	-	280	-	-	-	[36]
EV	18-41	1.01-1.42	0.6-2.4	20-300	-	HZ	3-8	[37]
EV	-	1-1.033	1.45-1.65	100-400	-	MP	-	[38]

Technique	GS/nm	[Sn/S]	E_g/eV	T_S/°C	T_{ann}, Atm/°C	Structure	RMS/nm	Reference
EV	-	0.9-1.6	1.5-1.7	100-400	-	MP	-	[39]
CBD	-	-	0.82-1.22	75	-	HZ	-	[40]
HI	2.7-4.8	~1	1.1-1.72	120	-	HZ	-	[41]
SP	9-12	1.18-1.47	1.3-2.3	300-500	-	HZ	-	[42]
CBD	20-24	~1.49	0.62-1.97	60	-	HZ	-	[43]
EV	32	~1.06	1.92	300	-	HZ	2.5-11	[44]
EV	30-50	0.97-2.92	1.33-1.53	250	200-400	HZ	-	[45]
EV	23-52	1.01-1.1	1.19-1.26	150-350	-	HZ	10-90	Present Study

GS: Grain Size, Atm:Atmosphere, SC: Single Crystal, CVD:Chemical Vapor Deposition, EV: Thermal Evaporation, EBE: Electron beam evaporation, cEV: Co evaporation, CBD: Chemical bath deposition, SILAR:, TD: Thermal decomposition, HI: Hot Injection, SP: Spray Pyrolysis, MP: Mixture of phases, HZ: Herzenbergite, VAC: Vacuum, A: Amorphous, PC: Partially Crystalline

2. Experimental procedure

SnS thin films were grown on soda lime glass and SnO_2:F coated glass substrates by the vacuum evaporation technique using 99.999 % pure tin sulfide powder (SnS). The base pressure of the evaporation chamber was $1x10^{-6}$ Torr, the powder sample was evaporated at a film deposition rate of 15 Å/s, the rate of the deposition was maintained constant at 15 cm, we applied a constant current of the 36 A and a voltage of the 2.25 V. The substrates were first cleaned with detergent and preserved in a chromic solution prepared with potassium dichromate and sulfuric acid for 12 h, after this the substrates were washed and exhaustively rinsed with deionized water, dried with nitrogen gas under pressure and stored in pure ethanol. Prior to loading in the vacuum chamber the substrates were dried under pressured nitrogen. The structural studies were performed using a Rigaku XRD system at a glazing incidence angle of 0.05. The Raman spectra technique was also used in a Labram Dilor. The morphological features were investigated using a Hitachi S5500 FESEM. The optical properties of the films were studied using a Lambda II UV-VIS spectrophotometer, and the Photoconductivity measurements were performed with a homebuilt system. In order to measure the photoconductivity two indium electrodes each of 3x9 mm area separated at a distance of 2 mm were vacuum evaporated on the film surface. Spectroscopic ellipsometry (SE) data in the photon energy range of 1.5 to 5.0 eV at the angle of incidence of 70° were acquired with an Uvisel system (Horiba-Jobin Yvon, Inc.). Transmittance spectra at normal incidence were obtained with a Perkin Elmer instrument in the range of 500 to 1100 nm.

3. Results and discussion

3.1. Properties of the films deposited at different substrate temperatures.

The deposited films were smooth, highly adherent to the substrate and free of pinholes when the substrate temperature was in the range of 150 to 350 ^oC. However, the films deposited below 150 ^oC showed poor adherence, the films deposited at temperatures above 350 °C were very thin and did not completely covered the substrate, which is why results are not presented. In the Figure 1 we are shown the Raman spectra of the films of the SnS grown at different substrates temperatures. The spectra show bands in 62.02, 92.38, 157.87, 184.84, 220.11 and 257.57 cm^{-1}.

Only the films grown at substrate temperature of 150 °C show 308.57 cm^{-1} additional vibrational band. In the literature we can find the Raman vibrational modes of the SnS as 96, 163, 189, 220, 288 cm^{-1} for Sn_2S_3 52, 60, 71, 183, 234, 251, 307 cm^{-1} and SnS_2 215, 315 cm^{-1} [46, 47] with oxidations states for the tin of the 2+, 3+ and 4+ respectively. Using the Raman spectra we find the presence of the SnS phase, additional vibrational modes at 62.02, 68.35 and 308.57 cm^{-1} can be due to the presence of traces of Sn_2S_3 and SnS_2 respectively.

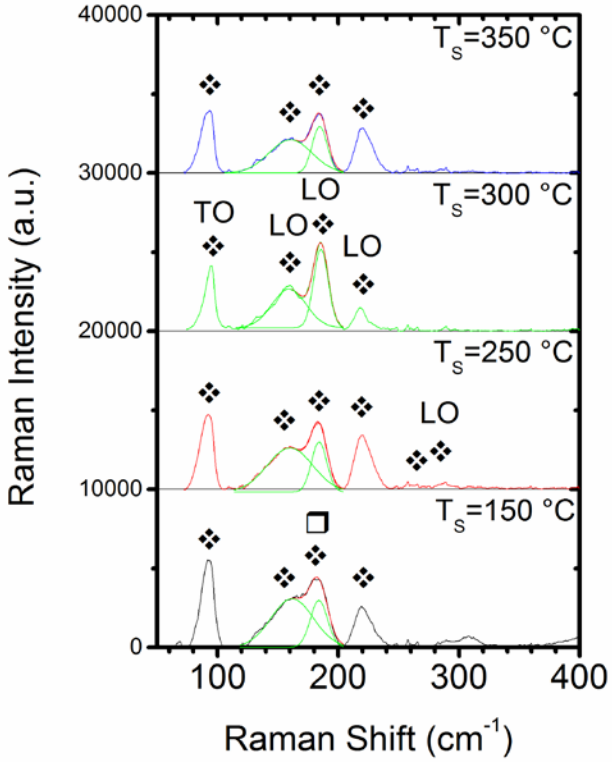

Fig.1 Raman spectra of the SnS thin film recorded in the wave number spectral range of 50 to 400 cm^{-1}. In the figure show ❖SnS and ❒Sn_2S_3 compounds.

Fig. 2 shows the diffraction patterns of the films grown at different substrate temperatures. The tin sulfide films exhibited orthorhombic structure similar to that of the mineral Herzenbergite. The strongest peak at 31.8^o indicates that the SnS film is preferentially oriented along the (111) plane. The X-ray pattern of the films deposited at all these substrate temperatures showed only the presence of SnS phase. The films grown at all the substrate temperatures reported in this work showed the presence of only one principal phase (SnS) on contrary to what was reported by Devika et al [20, 21], where SnS_2 and Sn_2S_3 phases were also observed. By Raman result only traces of the Sn_2S_3 and SnS_2 we can observe. In the Devika work, grown the SnS by the evaporated technique and varied from room temperature to 325 °C at 10 Å/s with a constant voltage of the 32 V with current of the 75 A. Others authors that have been grown SnS by different techniques, Hot Injection Technique [10], Spray Pyrolysis [11, 12], Electron Beam Evaporation [13], Evaporation [14], Chemical Bath Deposition [15,16], SILAR method [17,18] and Electrodeposition [19] are obtained principally SnS phase.

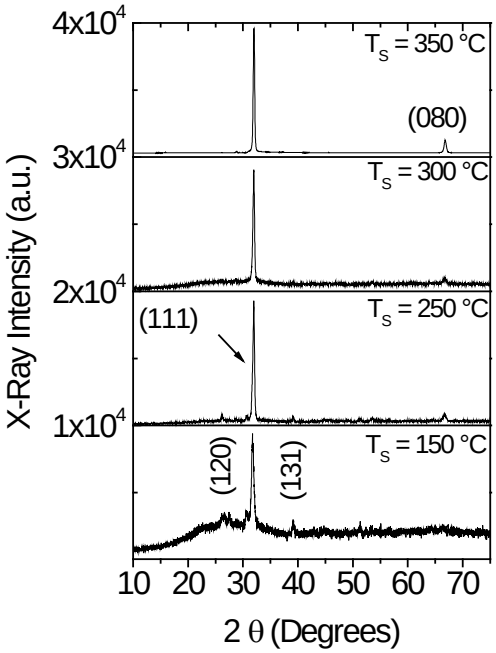

Fig.2 X-ray diffraction patterns of the SnS thin films grown at different substrate temperatures.

The average crystalline size of the SnS films was calculated from the predominant XRD peak (111) using the Scherer equation $D = \frac{k\lambda}{\beta cos\theta}$ where k = 0.90 the shape factor which is a constant, D is the crystallite size, λ is the wavelength of the incident radiation, θ is the Bragg angle taken in radians and β is the FWHM in radians. β^2 = (FWHM)^2−b^2, where b is the line breadth estimated using a powder sample of lanthanum hexaboride . The grain size increased with the substrate temperature, which is evident from the decrease in the full width at a half maximum (FWHM) of the (111) peak. Fig 3 shows the grain size plotted against substrate temperature. The grain size increased from 22 to 50 nm when the substrate temperature increased from 150 to 350 ^{o}C .

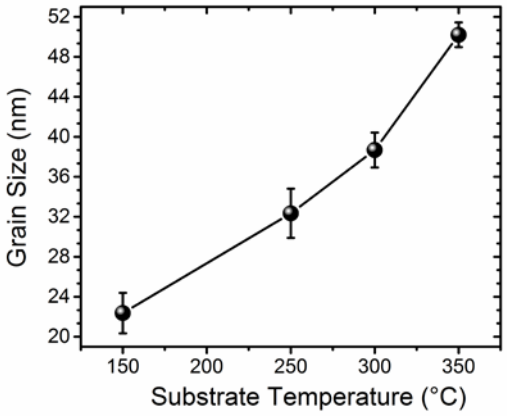

Fig. 3 Grain sizes of the SnS films versus substrate temperatures.

The lattice parameters for the orthorhombic phase were evaluated using the standard equation (1)

$$\frac{1}{d^2} = \frac{h^2}{a^2} + \frac{k^2}{b^2} + \frac{l^2}{c^2} \quad (1)$$

Where *h*, *k*, and *l* are the lattice planes and *d* is the interplanar distance and using the XRD data for the films deposited in the range of 150-350 ºC, these values are shown in the table II, we can observe that the unit-cell parameter for the powder of the SnS with a/c = 1.086. According with this table, the lattice parameters exhibit a more pronounced change as the temperature of substrate increases. The closest value of the unit-cell parameters to the value of the powder is the SnS thin film with the substrate temperature at 250 ºC with a ratio of a/c= 1.081 and the farther is for the SnS thin film grown at 350 ºC substrate temperature with a ratio a/c= 1.254.

Table II. The unit-cell parameters of the SnS as a function of the substrate temperature

Ts/°C	a/ Å	b/ Å	c/ Å	a/c
Powder	4.3255	11.1982	3.9842	1.086
150	4.1755	11.0534	4.072	1.025
250	4.259	11.2831	3.9409	1.081
300	4.5958	11.1944	3.7097	1.239
350	4.6332	11.4769	3.6947	1.254

The texture coefficient was determined in order to find the preferential orientation of the crystals in the polycrystalline SnS thin films. This factor can be compute from X-ray diffraction results using the following relation (2):

$$T_{(hkl)} = \frac{I_{m(hkl)}}{I_{0(hkl)}} \left(\frac{1}{N} \sum_1^N \left(\frac{I_{m(hkl)}}{I_{0(hkl)}} \right) \right)^{-1} \quad (2)$$

Where $I_{m(hkl)}$ is the measured relative intensity of the reflection from the (hkl) plane, $I_{0(hkl)}$ is that from the same plane in standard reference sample listed in the PDF#39-0354 database, N is the number or reflection peaks from the film. For a film to have a preferential orientation at any (hkl) plane, the texture coefficient must be at least one [48, 49]. From the results of the textured coefficient calculations for different planes, it was found that the preferential orientation of deposited films with different substrate temperatures was the (111) plane the figure 4 shows the graph of the texture coefficient versus the planes of the XRD patterns of the thin films grown at different substrates temperatures.

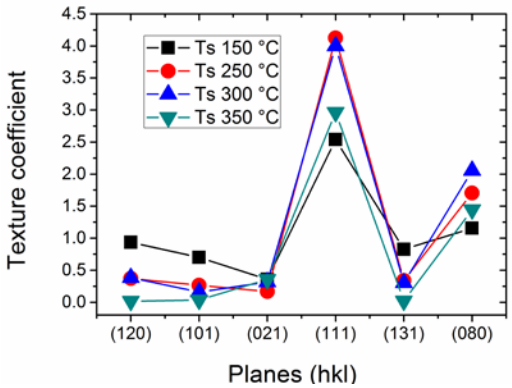

Fig. 4 Texture coefficient of the SnS films grown varying substrate temperatures.

The strain was calculated using the FWHM´s that can be expressed as a linear combination through the following equation (3):

$$\frac{\beta cos\theta}{\lambda} = \frac{1}{\varepsilon} + \frac{\eta \, sin\theta}{\lambda} \quad (3)$$

Where β is the measured FWHM in radians, θ is the Bragg angle of the diffraction peak, λ is the x-ray wavelength, ε is the effective particle size, and η is the effective strain. In the figure 5 we observed a strain versus substrate temperature of the SnS thin films, the lower strain is for the thin films grown at a substrate temperature of the 250ºC and increase as the substrate temperature increase. The SnS thin film grown at 150ºC exhibit the highest value of the strain, this could be due to the low temperature of the substrate and consequently the low mobility of atoms to have a better arrangement in the polycrystal.

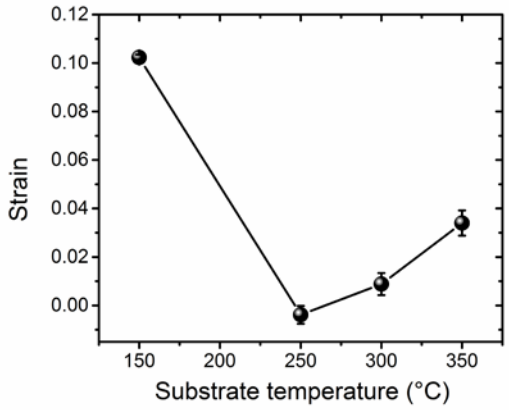

Fig. 5. Strain versus SnS thin films substrate temperature

The SEM studies on SnS thin films show the clear dependence of surface morphology on the substrate temperature. Images of the films deposited at 150, 250, 300 and 350 °C substrate temperatures are shown in Fig. 6. In general the films exhibit very compact and uniform surfaces with elongated grains. The grain growth is significantly is promoted by substrate temperature, which is in agreement with the trend observed in the XRD data.

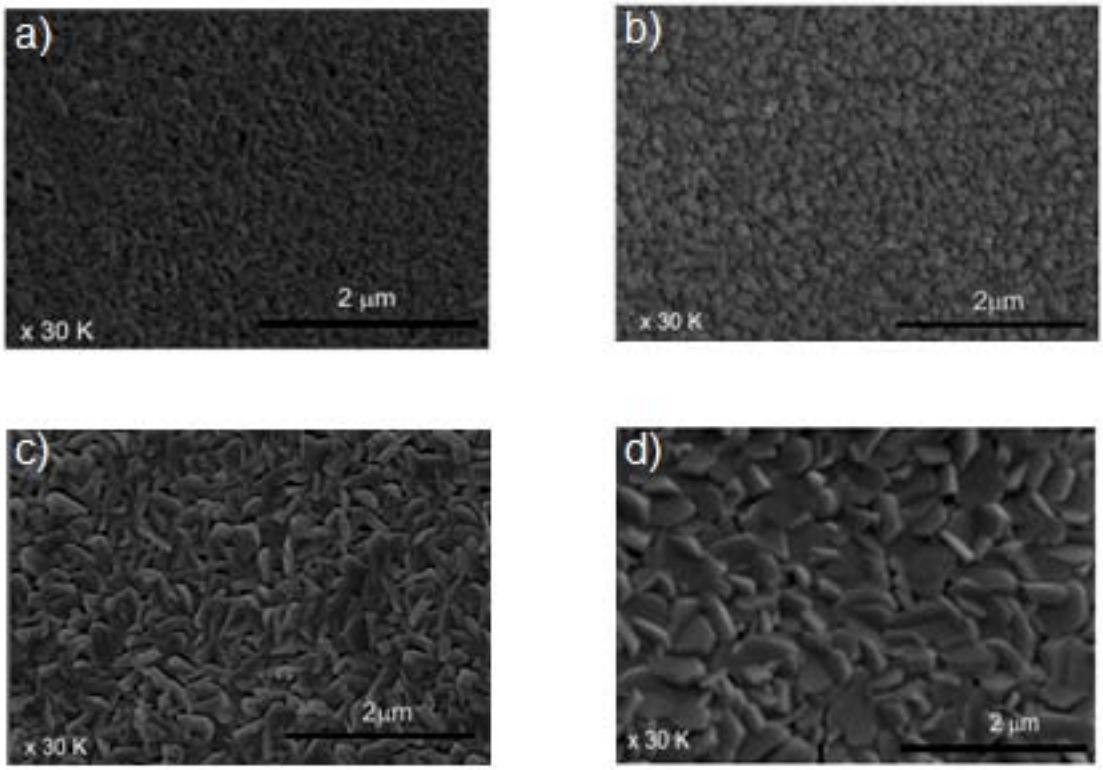

Fig. 6. SEM images as a function of substrate temperature of the SnS at a) 150, b) 250, c) 300 and d) 350°C.

The EDS analysis of SnS thin films showed that the tin and sulfur composition in the films, in general varied with the increase of the substrate temperature. The Fig 7 shows the variation of Sn and S atomic ratio versus substrate temperature, which indicates the loss of sulfur content in the films with the increase of temperature. The film grown at 150 °C is Sn rich deficient in sulfur with Sn/S atomic ratio of 1.068, with the increase of the substrate temperature to 250 °C this film is very close to the stoichiometric with Sn/S atomic ratio of 1.015, at higher substrates temperatures the films become nonstoichiometric (see Fig. 6) this change in the stoichiometry is probably due to the re-evaporation of the sulfur because of its high vapor pressure at this substrate temperature and vacuum characteristics.

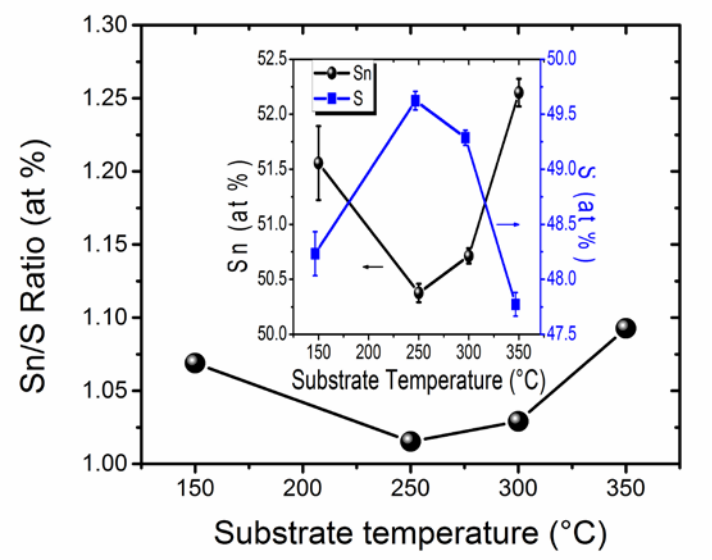

Fig 7 EDS characterization of the SnS films grown by varying the substrate temperature. Inset; atomic percentage of Sn and S versus substrate temperature

The optical properties of the films were studied from the transmittance spectra of the films recorded in the wavelength range 300 to 2500 nm. The variation of the refractive index (n), extinction coefficient (k) and band gap (E_g) of the films with respect to the deposition temperature is shown in Fig. 9. The values of n, k, and α were estimated using the equations (4) to (7) given below.

$$\alpha h\nu = A(h\nu - E_g)^n \tag{4}$$

Where n is 2 and 2/3 respectively for direct allowed and forbidden transitions, and n is ½ for indirect allowed transitions and 1/3 for indirect forbidden transitions. The plot of the $(\alpha h\nu)^{2/3}$ vs hν with the linear portion we obtained the band gap see inset of the figure 8.

$$n = \left[N + (N^2 - n_0^2 n_1^2)^{1/2}\right]^{1/2} \tag{5}$$

$$\text{Here } N = \frac{(n_0^2+n_1^2)}{2} + 2n_0n_1\frac{(T_{max}-T_{min})}{T_{max}T_{min}} \tag{6}$$

Where n_1 is the refractive index of air, n_2 the refractive index of the substrate, T_{max} and T_{min} are the maximum and minimum transmission respectively at a given wavelength. The extinction coefficient k of the as deposited SnS films was evaluated using the equation (7).

$$k = \frac{\alpha\lambda}{4\pi} \tag{7}$$

Where α is the absorption coefficient and λ the wavelength. The results are presented in the table III

Table III. Refractive index as a function of substrate temperature

T_s/°C	n	k
150	3.057	0.0341
250	3.100	0.0201
300	3.005	0.0655
350	3.360	0.0114

The average value of the refractive index as a function the substrate temperature is 3.13, and increase as the temperature of substrate increase. The extinction coefficient of the as deposited films of the SnS was evaluated using equation (7), initially increased with the increase of the substrate temperature with a maximum value of the 0.0655 at T_s=300 °C, for the substrate temperature of the 350 °C the value decrease at 0.0114. Similar results were reported by El-Nahass et. al. [14] by thin films of the SnS thermally evaporated.

The band gap increased from 1.19 to 1.25 eV when the substrate temperature increased from 150 to 300 ^{o}C. The observed increase in band gap in the temperature range 150 to 300 ^{o}C can be explained as due to the increase in grain size (Fig. 3). This can be either due to a change in film stoichiometry, or recrystallization leading to grain fracturing, or formation of traces of the other phases of tin sulfide such as SnS_2 and Sn_2S_3, The shift in energy band gap with deposition conditions has been observed by other researchers. These researches attribute the change in the optical absorption edge to the low presence of other phases of tin sulphide i.e. Sn_2S_3 (E_g=2.0 eV) and SnS_2 (E_g=2.44 eV). The inset of Fig. 8 shows the compute of the gap of the SnS thin film for a substrate temperature of 300 °C.

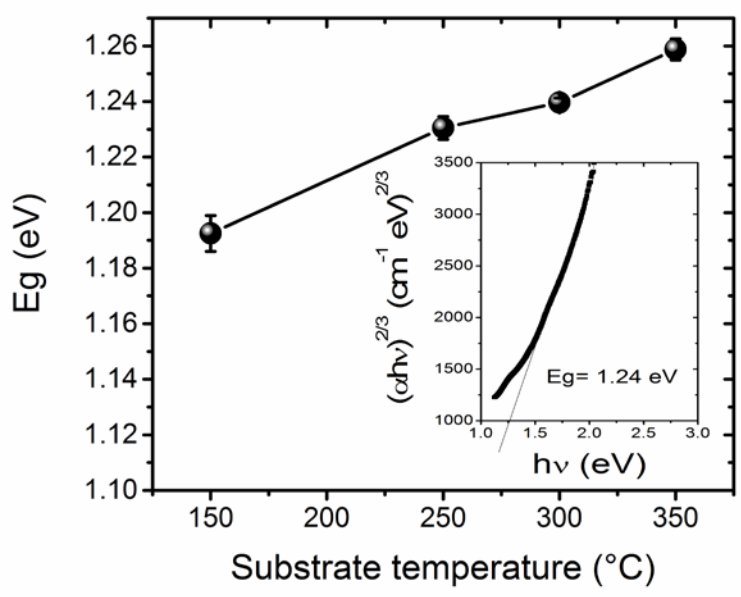

Fig. 8. Shows band gaps of the SnS thin films versus substrate temperature.
The Inset is the Tauc plot in the case of the substrate temperature of the 300 °C

Fig. 9 shows the experimental and best fit of transmittance (a) and ellipsometric spectra. The best fit was obtained considering an air-roughness-SnS film-glass substrate system. A generalized Lorentz harmonic oscillator model represented the SnS film dielectric function. The roughness was the modeled with the Bruggeman effective medium approximation using a 50%-50% mixture of voids and SnS. The film thickness determined from the fitting procedure was 480 nm and a roughness 16 nm. In Fig. 9(a) and (b) it can be observed that the fitted spectra give a very good description of the measured spectra.

The absolute values shown by $\varepsilon_{\|eff}$ in Fig. 9(c) are lower but comparable to the reported for SnS single crystal [50]. The arrows drawn in Fig. 9(c) locate interband transitions, which are also in agreement with those for single crystal [50] and theoretical calculations [51,52]. The refractive index reported of thermally evaporated SnS films is about 3 at wavelengths larger than 1000 nm [53], and films deposited by chemical bath show an even lower refractive index [54].

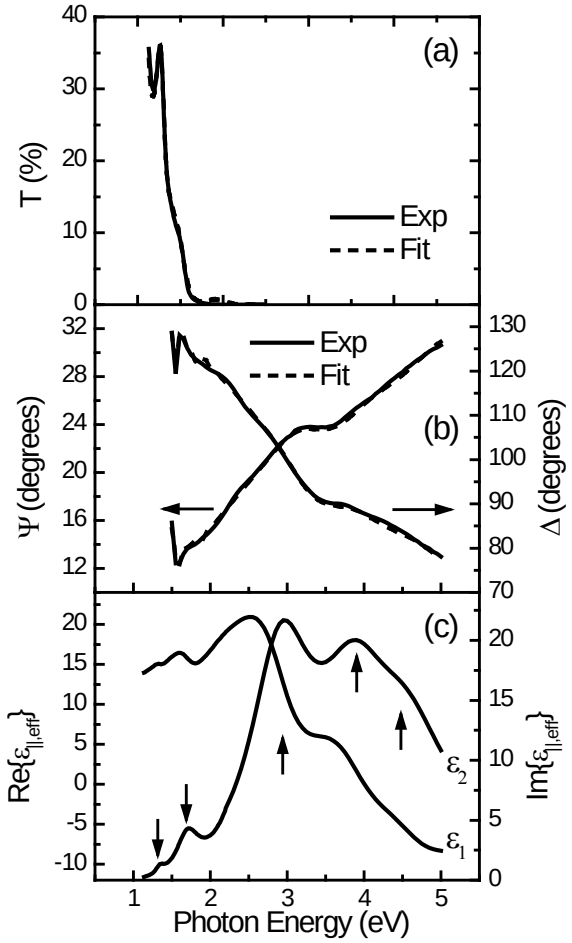

Fig. 9. (a) Experimental and best fit spectra of normal incidence transmittance (a), ellipsometric angles Ψ and Δ (b). (c) Averaged dielectric function $\varepsilon_{\|eff}$, Eq. (1) of SnS film

The conductivity of the films is measured in the dark and under illumination by applying a constant potential of 10 V. After applying the bias, the films are kept in the dark for sufficient time to stabilize the current. Once the current is stabilized a program is initiated to monitor the current on-line at regular intervals before, during, and after a light pulse. Fig. 10(a) shows the conductivity measured in the dark and under illumination, and Fig. 10(b) is the resistivity value computed using the data in (a). All the films are photosensitive and show a noticeable dependence on the substrate temperatures. Films deposited at lower temperatures have exhibit transient current in the dark after illumination indicating the presence of trap states in the band gap of the material.

The photosensitivity S of a material is defined as $S = (I_l - I_d)/I_d$, where I_l is the current under illumination and I_d is the current measured in the dark. The computed values of the photosensivity and resistivity are shown in the Fig. 10(b). It can be observed from Fig.1 to Fig. 9 that the band gap, photoresponse, film resistivity, and photosensitivity are strongly dependent on the film deposition temperature, and at 300 ^{o}C all these parameters shows a very significant deviation, the deviation could be attributed at the increase in the tin concentration for a sample of T_s= 350 °C.

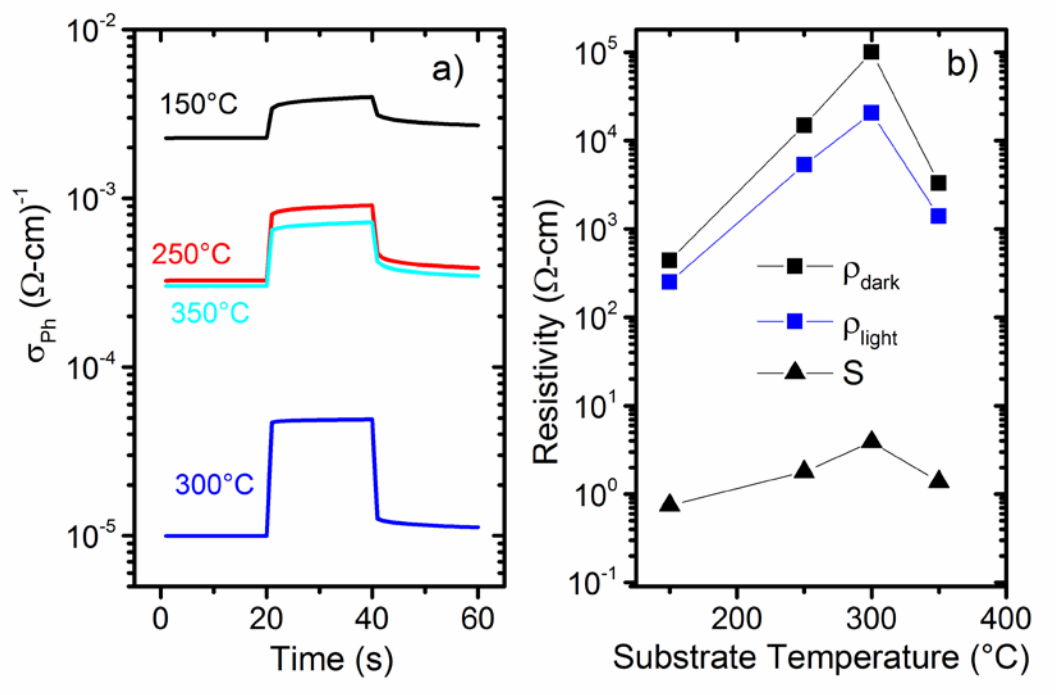

Fig. 10: (a) Photocurrent response and b) resistivity values of SnS at deposited at different substrate temperatures and photosensitivity

4. Conclusions

Thin sulfide thin films can be grown by physical evaporation of powder of SnS at deposition temperatures from 150 up to 350 °C. The Raman studies showed a SnS phase with traces of Sn_2S_3 and SnS_2. XRD studies confirmed the Herzenbergite, orthorhombic structure with lattice parameters a/c equals to 1.086 and 1.081for the powder and for the substrate temperature of 250 °C respectively. All samples were preferentially oriented (111) plane. The average crystallite sizes estimated from XRD data were 22 to 49 nm. The strain was minimum for the sample grown at 250°C substrate temperature. The atomic ratio Sn/S from EDS-SEM was for the film growth at 250 °C closer to the stoichiometry with ratio equal to 1.015. The optical band gaps of SnS films were 1.19 up to 1.25 eV. The films exhibited photoresponse and with the resistivity values in the dark were $2x10^2$ up to $1x10^5$ Ω-cm.

Acknowledgements

We thank Projects ICyTDF, CONACYT-0111299, CONACyT 129169, CONACYT-SENER-117891 and CONACYT-154787.

References

[1] T. Jiang, G. A. Ozin., J. Mater. Chem. **8**, 1099 (1998).
[2] Robert W. Miles, Ogah E. Ogah, Guillaume Zoppi, Ian Forbes., Thin Solid Films **517,** 4702 (2009).
[3] M. Calixto-Rodriguez, H. Martinez, A. Sanchez-Juarez, J. Campos-Alvarez, A. Tiburcio-Silver , M.E. Calixto., Thin Solid Films **517**, 2497 (2009).
[4] Naoya Sato, Masaya Ichimura, Eisuke Arai, Yoshihisa Yamazaki., Solar Energy Materials & Solar Cells **85,** 153 (2005).
[5] A. Tanuisevski, D. Poelman, Sol. Energy Mater. Sol. Cells **80**, 297 (2003).

[6] H. Noguchi, A. Setiyadi, H. Tanamura, T. Nagatomo, O. Omoto, Sol. Energy Mater. Sol. Cells **35,** 325 (1994).
[7] J.P. Singh, R.K. Bedi, Thin Solid Films **199**, 9 (1991).
[8] J. J. Loferski, J. Appl. Phys., **27**, 777 (1956).
[9] PDF Card #39-0354
[10] Dmitry S. Koktysh, James R. McBride, Robert D. Geil, Benjamin W. Schmidt, Bridget R. Rogers, Sandra J. Rosenthal., Materials Science and Engineering B **170**, 117 (2010).
[11] N. Koteswara Reddy, K.T. Ramakrishna Reddy., Thin Solid Films **325**, 4 (1998).
[12] T. H. Sajeesh, Anita R. Warrier, C. Sudha Kartha, K.P. Vijayakumar.,Thin Solid Films., **518**, 4370 (2010).
[13] A. Tanusevski, D. Poelman., Solar Energy Materials & Solar Cells **80**, 297 (2003).
[14] M.M. El-Nahass, H.M. Zeyada, M.S. Aziz, N.A. El-Ghamaz., Optical Materials **20**, 159 (2002)
[15] David Avellaneda, M.T.S. Nair, P.K. Nair., Thin Solid Films **517**, 2500 (2009)
[16] Yu Wang, Y. Bharath Kumar Reddy, Hao Gong., J. Electrochem. Soc., **156**(3), H157 (2009).
[17] Chao Gao, Honglie Shen, Tianru Wu, Lei Zhang, Feng Jiang., Journal of Crystal Growth **312,** 3009 (2010).
[18] Chao Gao, Honglie Shen, Lei Sun, Haibin Huang, Linfeng Lu, Hong Cai., Materials Letters **64,** 2177 (2010).
[19] Shuying Cheng, Yanqing Chen, Yingjie He, Guonan Chen., Materials Letters **61,** 1408 (2007).
[20] M. Devika, K. T. Ramakrishna Reddy, N. Koteeswara Reddy, K. Ramesh, R. Ganesan, E.S.R. Gopal and K.R. Gunasekhar., J. Appl. Phys., **100**, 023518 (2006)
[21] M. Devika, N. Koteeswara Reddy, K. Ramesh, K.R. Gunasekha E.S.R. Gopal K. T. Ramakrishna Reddy., Semicond. Sci. Technol., **21,** 1125 (2006).
[22] H.R. Chandrasekhar, R.G. Humphreys, U.Zwick and M. Cardona., Physical Review B., **15**(4), 2177 (1977).
[23] R. D. Engelken, H. E. McCIoud, Chuan Lee, Mike Slayton and Hossein Ghoreishi., J. Electrochem. Soc., **134(**11), 2696 (1987).
[24] M.M. El-Nahass, H.M. Zeyada, M.S. Aziz, N.A. El-Ghamaz., Optical Materials **20,** 159 (2002).
[25] A. Tanusevski, D. Poelman., Solar Energy Materials & Solar Cells **80,** 297 (2003).
[26] A. Abou Shama, H.M. Zeyada., Optical Materials **24**, 555 (2003).
[27] H. A. Hashem, and S. Abouelhassan., Chinese journal of physics., **43**(5), 955 (2005).
[28] M Devika, N Koteeswara Reddy, K Ramesh, H R Sumana, K R Gunasekhar, E S R Gopal K T Ramakrishna Reddy., Semicond. Sci. Technol. **21**, 1495 (2006).
[29] C. Cifuentes, M. Botero, E. Romero, C. Calderón, and G. Gordillo., Brazilian Journal of Physics., **36**(3B), 1046 (2006).
[30] M. Devika, N. Koteeswara Reddy, K. Ramesh, K. R. Gunasekhar, E. S. R. Gopal, K. T. Ramakrishna Reddy., Journal of The Electrochemical Society, **153(**8), G727 (2006).
[31] N. koteeswara reddy, k. Ramesh, R. ganesan, k.t. ramakrishna reddy, k.r. gunasekhar, E.S.R. Gopal., Appl. Phys. A **83**, 133 (2006).
[32] M. Devika, N. Koteeswara Reddy, K. Ramesh, R. Ganesan, K. R. Gunasekhar, E. S. R. Gopal, K. T. Ramakrishna Reddy., Journal of The Electrochemical Society., **154**(2) H67 (2007).
[33] M. Devika, N. Koteeswara Reddy, D. Sreekantha Reddy, S. Venkatramana Reddy, K. Ramesh, , E. S. R. Gopal, K. R. Gunasekhar, R. Ganesan, Y.B. Hahn., J. Phys: Condens. Matter, **19**, 306003 (2007).
[34] D. Avellaneda, G. Delgado, MTS Nair and PK Nair., Thin Solid Films., **515**, 5771 (2007).
[35] B. Ghosh, M. Das, P. Banerjee and S. Das., Appl. Surf. Sci. **254**, 6436 (2008).
[36] Jung-wook Seo, Jung-tak Jang, Seung-won Park, Chunjoong Kim, Byungwoo Park Jinwoo Cheon., Adv. Mater., **20**, 4269 (2008).
[37] M. Devika, N. Koteeswara Reddy, D. Sreekantha Reddy, Q. Ahsanulhaq, K. Ramesh, E. S. R. Gopal, K. R. Gunasekhar, Y. B. Hahn., J. Electrochem. Soc., **155** 2, H130 (2008).

[38] Ogah E. Ogah, Guillaume Zoppi, Ian Forbes, R.W. Miles., Thin Solid Films., **517,** 2485 (2009).
[39] Robert W. Miles, Ogah E. Ogah, Guillaume Zoppi, Ian Forbes., Thin Solid Films., **517,** 4702 (2009).
[40] Y. Wang, Y.B.K. Reddy and Hao Gong., *J. Electrochem. Soc.*, **156**(3) H157 (2009) .
[41] D. S. Koktysh, J. R. McBride, R. D. Geil, B.W. Schmidt, B.R. Rogers, S.J. Rosenthal., Mat. Sci. and Eng. B, **170**, 117 (2010).
[42] T.H. Sajeesh., A.R. Warrier, C.S. Kartha, K.P. Vijayakumar., Thin Solid Films., **518,** 4370 (2010).
[43] E. Guneri, C. Ulutas, F. Kirmizigul, G. Altindemir, F. Gode, C. Gumus., Appl. Surf. Sci., **257**(4), 1189 (2010).
[44] M. Devika, N. Koteeswara Reddy, M. Prashantha, K. Ramesh, S. Venkatramana Reddy, Y. B. Hahn and K. R. Gunasekhar., Phys. Status Solidi A **207(**8), 1864 (2010).
[45] Biswajit Ghosh, Rupanjali Bhattacharjee, Pushan Banerjee, Subrata Das., Applied Surface Science., (2010) doi:10.1016/j.apsusc.2010.11.103.
[46] Louise S. Price, Ivan P. Parkin, Amanda M. E. Hardy, Robin J. H. Clark, Thomas G. Hibbert, Kieran C. Molloy., Chem. Mater. **11**(7), 1792 (1999).
[47] I. P. Parkin, L. S. Price, T. G. Hibbert and K. C. Molloy. J. Mater. Chem. **11**, 1486 (2001).
[48] Nair J.P., Jakakrishna R., Chaure N.B., Pandey R.K., letter to the editor, Semicond Sci. Technol., **13,** 340 (1998)
[49] Guneri E., Gumus C., Mansur F., Kirmizigul F., Optoelectron. Adv. Mater. Rapid. Commun. **3**, 383 (2009).
[50] R. Eymard, A. Otto, Phys. Rev. B **16**, 1616 (1977).
[51] Z. Nabi , A. Kellou, S. Mécabih, A. Khalfi, N. Benosman, Materials Science and Engineering B **98,** 104 (2003).
[52] L. Makinistian and E. A. Albanesi, Phys. Status Solidi B **246**, 183 (2009).
[53] M.M. El-Nahass, H.M. Zeyada, M.S. Aziz, N.A. El-Ghamaz, Optical Materials **20,** 159 (2002).
[54] E Turan, M Kul, A S Aybek, M Zor, J. Phys. D: Appl. Phys. **42,** 245408 (2009).